Available online at www.sciencedirect.com
ScienceDirect
Surgical Neurology 72 (2009) S1:8 – S1:16
SURGICAL NEUROLOGY
www.surgicalneurology-online.com

Genetics

Hammerhead ribozyme targeting human hypoxia inducible factor-1α gene effectively attenuates HeLa xenograft tumors

Rutong Yu[c,*,1], Rui Chen[e,1], Qiong Shi[c], Ting Li[d], Hong Tang[a,b]

[a]Center for Molecular Immunology, The Institute of Biophysics, Chinese Academy of Sciences, Beijing 100080, China
[b]The Institute of Microbiology, Chinese Academy of Sciences, Beijing 100080, China
[c]Department of Neuronal Surgery, The Affiliated Hospital of Xuzhou Medical College, Xuzhou 221002, China
[d]Department of Pathology, Xuzhou Medical College, Xuzhou 221002,China
[e]Beijing Tongren Hospital, 100730, China

Received 23 August 2007; accepted 20 February 2008

Abstract

Background: Hypoxia inducible factor l is a heterodimeric transcription factor that plays an important role in oxygen homeostasis. A good body of evidence indicates that overexpression of HIF-1α driven by intratumoral hypoxia can transactivate genes essential for energy metabolism, erythropoiesis, and vascular development, which is directly involved in cancer progression. Overexpressed HIF-1α also has a considerably reversed clinical correlation with treatment efficacy as well as mortality of cancers.

Methods: We took the advantage of the hammerhead ribozyme that specifically targeted 1762-1778 nt of HIF-1α messenger RNA.

Results: The designed ribozyme could cleave its substrate HIF-1α messenger RNA in both in vitro and in intracellular cleavage assays. More interesting, the synthetic ribozyme RNA administered to HeLa xenograft large tumor could effectively inhibit its angiogenesis and tumor growth.

Conclusion: It is reasonable to speculate that down-regulation of HIF-1α activity could be a potential mechanism useful to prevent survival or angiogenic activity of various solid tumors.
© 2009 Elsevier Inc. All rights reserved.

Keywords: HIF-1; Ribozyme; Cancer; Gene therapy

1. Introduction

Oxygen homeostasis plays an important role in development and physiology and individual cell sense and respond to changes in oxygen availability via transcriptional induction of genes involved in energy metabolism, hematopoiesis, angiogenesis, invasion and vascular tone, development, and remodeling [4,22]. Disruption of this delicate adaptation to the hypoxic stress is usually associated with cardiovascular disorders, ischemia, and cancer [23]. One of the important sensor and regulator of tissue oxygenation status is HIF-1, which is a heterodimeric basic helix-loop-helix PAS transcription factor consisting of HIF-1α and HIF-1β/Arnt subunits [15,33], and the heterodimer binds to the HRE (5′[G/C/T]-ACGTGC-[G/T]) present in promoters and enhancers of many target genes [25,26]. Hypoxia inducible factor l is stabilized in response to hypoxia and rapidly degraded under normoxic conditions. In contrast to HIF-1β, which is constitutively expressed, HIF-1α protein synthesis is regulated in an O_2-independent manner, whereas HIF-1α protein degradation is controlled in an O_2-dependent fashion that involves prolyl hydroxylation of HIF-1α by Egl-9 and subsequent pVHL-dependent ubiquitination and proteasomal degradation [16,20,22]. On the other hand, HIF-1α transcription activity

Abbreviations: CMV, cytomegalovirus; DMEM, Dulbeco's modified eagle medium; HIF-l, hypoxia inducible factor l; HRE, hypoxia-responsive element; mRNA, messenger RNA; mRz, mutant ribozyme; PAS, Per/Arnt/Sim; PBS, phosphate buffer solution; PCR, polymerase chain reaction; PVHL, Von Hippel-Lindau suppressor gene protein; RLU, relative luciferase activity; Rz, ribozyme; VEGF, vascular endothelial growth factor.

* Corresponding author. Tel.: +86 156 85802496; fax: +86 156 85748431
E-mail address: sq56_2008@126.com (R. Yu).
[1] R.C. and R.Y. contributed equally to this work.

0090-3019/$ – see front matter © 2009 Elsevier Inc. All rights reserved.
doi:10.1016/j.surneu.2008.02.038

is also precisely regulated via O_2-dependent asparaginyl hydroxylation in hypoxic cells or O_2-independent mechanisms when cells are encountered with growth factor stimulation, gain-of-function oncogene products, or loss-of-function tumor suppressors [16,25]. A good body of evidence indicates that HIF-1α is directly involved in cancer progression driven by intratumoral hypoxia [11,25]. First, target genes encoding angiogenesis factors, invasion factors, glycolytic factors, and glucose transporters, which are involved in various stages of cancer metastasis, are regulated by HIF-1α [5,14,17,21]. Second, HIF-1α is overexpressed as a result of intratumoral hypoxia as well as genetic alterations in most common human cancers [31,34], and there is a considerable clinical correlation between HIF-1α expression level and treatment efficacy as well as mortality of quite a few cancers [25].

Given the central role that HIF-1α plays in compensation of loss of oxygen and promotion of concomitant angiogenesis and glycolysis, it is reasonable to speculate that down-regulation of HIF-1α activity could be a potent mechanism in prevention of survival or angiogenic activity of various solid tumors [10]. More important, numerous lines of evidence have already indicated that hypoxic cancer cells tend to resist radiation and chemotherapy, which are often mediated by overexpression of HIF-1α [1,32], and have a high risk of invasion, metastasis, and mortality [13]. Therefore, anti-angiogenesis therapies against cancers would benefit a lot by inhibition of HIF-1α activity. Indeed, several small molecules that are inhibitors of HIF-1 activity have already been screened and are under clinical evaluation [25]. The use of antisense oligonucleotides targeting HIF-1α alone or in combination with chemotherapy has also produced significant regression of various tumors [7,28,29].

Ribozymes are RNA molecules with highly specific intrinsic enzymatic activity against target RNA sequences, which can discriminate mutant sequences differing by a single base from their wild-type counterparts [6,30]. After binding to the RNA substrate by base pair complementation, the ribozyme cleaves the target RNA irreversibly then releases itself for new rounds of cleavage, resulting in significantly improved target/effector stoichiometry as compared with antisense oligonucleotides of the same specificity. Hammerhead ribozyme has been identified as the smallest ribozyme composed of roughly 30 nucleotides with a conserved catalytic domain in the single-stranded region and variable stem regions (stems I and III) formed by base-pairing with basically any desired target sequences [12,30]. The characteristic site-specific cleavage of a phosphodiester bond after uridine of the triplet NUY sequence (N is any nucleotide and Y is any nucleotide but G, whereas GUC is the optimal motif) of its substrate [27] thus provide a very valuable tool for gene therapy at the level of RNA-mediated inhibition of gene expression.

Considering the functional link between overexpression of HIF-1α and tumorigenesis, invasion and metastasis, and enzymatic advantage of ribozyme over antisense oligonucleotide strategies, we took the approach of the hammerhead ribozyme to specifically down-regulate HIF-1α gene expression. After its in vitro cleavage activities were confirmed, the synthetic ribozyme RNA was administered to cervical adenocarcinoma xenografts. With the reduction of intratumoral HIF-1α levels, we also observed effective inhibition of angiogenesis and tumor growth of HeLa tumors.

2. Results

2.1. In vitro cleavage activity of the ribozyme

There are 23 GUC triplets in the sequence of HIF-1α mRNA, which could serve as the potential cleavage sites for a ribozyme. Using the multiple alignment of HIF-1α mRNA from rat, mouse, and human, predictive model secondary structures of the full length and local segment mRNA was optimized using algorithm of minimal free energy [3]. Three potential substrate sequences at 72-88, 577-593, and 1762-1778 nt were scored with GUC triplet accessible to ribozyme

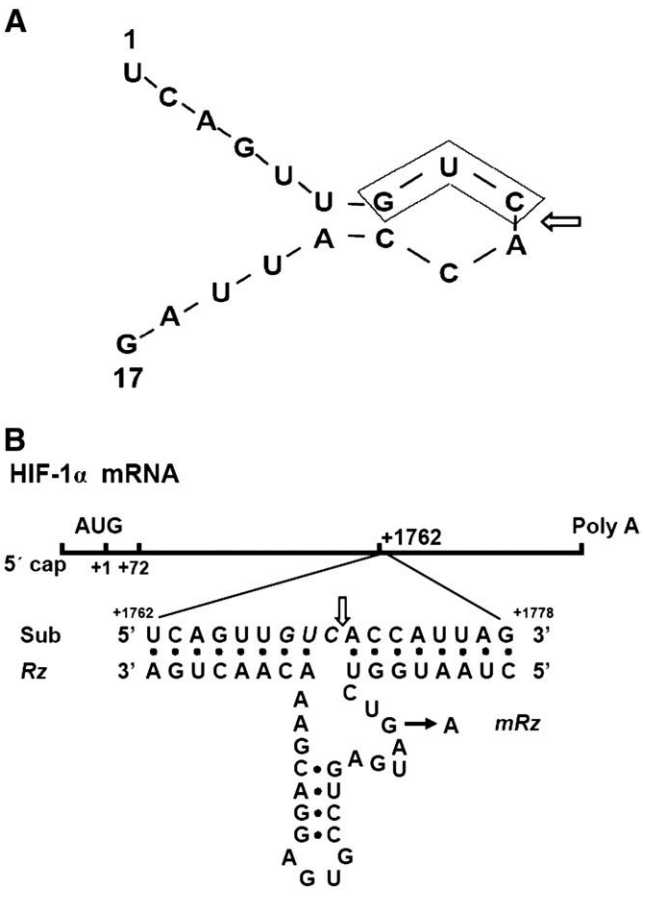

Fig. 1. Designing of HIF-1α ribozyme. A: The predicted secondary structure of the accessible substrate sequence (17 nt, 1762-1778 nt in HIF-1α mRNA) with the conserved GUC triplet in box. B: Schematic representation of the hammerhead ribozyme (Rz) directed against the HIF-1α mRNA. Non-catalytic ribozyme derivative (mRz) with G→A mutation was indicated. The putative cleavage site in the substrate was indicated by an arrow after the conserved GUC triplet. The base pairing in the stem structure of catalytic core and substrate recognition arms of the ribozyme was indicated by dots.

cleavage, and the representative substrate (designated as Sub) spanning from 1762 to 1778 of HIF-1α was shown (Fig. 1A). Ribozymes against these 3 potential substrate sequences were designed to achieve compromised maximal hammerhead catalysis according to rules set forth previously [8,12,18]. The representative ribozyme (designated as Rz), and its G11A mutant variant (mRz), against Sub was shown (Fig. 1B). The 8 base pair complementation flanking the GUC triplet was chosen for a favorable kinetics of substrate binding and product release. The other 2 ribozyme targeting 72-88 or 577-593 nt region of HIF-1α RNA showed similar or less effectiveness in the in vitro cleavage assays (data not shown).

To determine whether the designed ribozymes could exert specific catalytic activity, in vitro cleavage reactions were performed using α-^{32}P-CTP labeled Sub (Fig. 2A) as the substrate. The wild-type ribozyme generated from in vitro transcription could dissect Sub RNA to yield 2 products of predicted size (Fig. 2B), whereas the mRz failed to do so. This result strongly indicated that cleavage of HIF-1α Sub by designed ribozyme was specific and such specific cleavage was also dose-dependent in our multiple turnover reactions.

2.2. Intracellular cleavage activity of the ribozyme

To measure the intracellular or in vivo cleavage efficiency of a ribozyme against its target mRNA is the ultimate task in clinical application of ribozyme therapy. To determine whether the designed ribozyme could specifically down-regulate gene expression of HIF-1α, an HIF-1α mRNA reporter system was established in which the ribozyme substrate sequence of HIF-1α (1762-1778 nt) was embedded in the 3′ terminus of *Renilla luciferase* gene right before the polyadenosine tail (Fig. 3A, phRL-CMV/Sub). To effectively generate ribozyme RNA in cells, we took advantage of the pSUPER vector backbone in which the ribozyme expression was driven by the polymerase-III H1–RNA gene promoter, and the corresponding RNA transcript lacked a polyadenosine tail (Fig. 3A, pSUPER/Rz and its mutant derivative pSUPER/mRz). *Renilla luciferase* activity as an indicator of ribozyme activity was then measured by cotransfection of Sub and Rz expression vectors into HEK293T. Although mutant Rz mildly affected *Renilla luciferase* activities, expression of wild-type Rz effectively down-regulated the reporter activity in a dose-dependent manner (Fig. 3B). The partial inhibition of the reporter activity by mRz cotransfection raised a concern that substrate binding by the ribozyme mRz, thus a steric hindrance to polyadenosination, rather than substrate cleavage, could also be a factor to decrease reporter activity. However, more pronounced reduction of reporter activities by the wild-type Rz than by mRz suggested that catalytic effect of ribozyme rather than antisense effect of mRz would be more favorable intracellularly.

Hypoxia inducible factor 1α is directly involved in cancer progression driven by intratumoral hypoxia [11,25], and expression of VEGF induced by HIF-1α is linked to angiogenesis [9,24]. To determine whether the ribozyme could inhibit endogenous HIF-1α expression under hypoxic conditions and subsequently down-regulate VEGF expression, pSUPER/Rz and VEGF promoter reporter pGL3-VEGF-Luc were cotransfected into HeLa cells treated with cobalt chloride to mimic the hypoxic condition. Increased expression of Rz effectively inhibited HIF-1α expression as indicated in the immunoblotting assay using HIF-1α specific antibody (Fig. 4A, top panel). In the meantime, the same transfectants showed similar dose-dependent reduction of

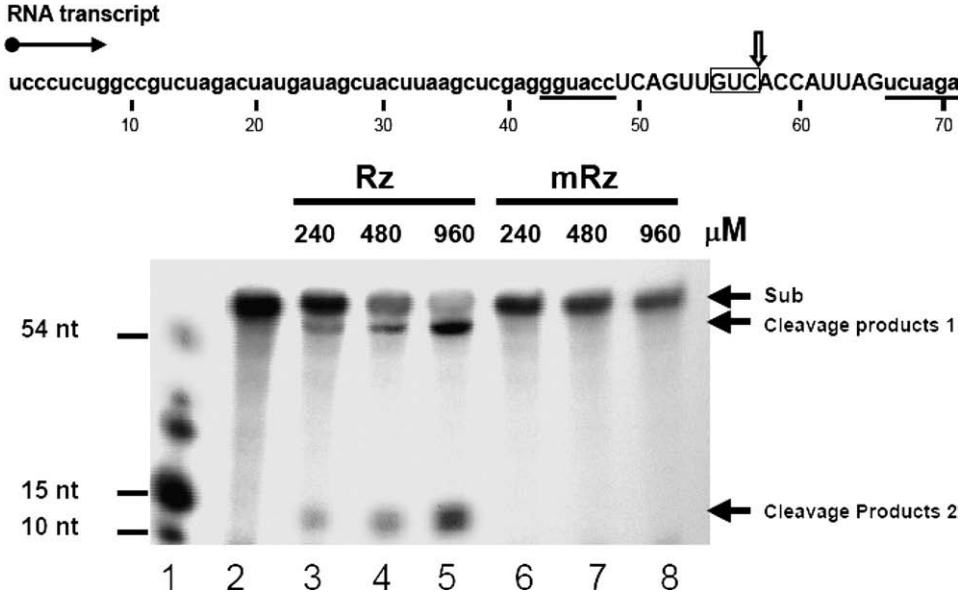

Fig. 2. Ribozyme in vitro cleavage assays. A: Schematic representation of the substrate sequence (upper cases) generated from pSP72-Sub vector in between Xba I and EcoR I sites (underlined) by in vitro runoff transcription reaction. Extra nucleotides flanking Sub in the transcript were indicated in lower cases. B: Fixed amount of Sub (80 μmol/L) was annealed to the increasing amounts of Rz or mRz (240, 480, and 960 μmol/L) in a total volume of 10 μL of 50 mmol/L Tris-HCl (pH 7.5). Cleavage reaction was initiated by addition of $MgCl_2$ and cleavage products (58 nt and 14 nt, respectively) were resolved in 20% PAGE/8 mol/L urea.

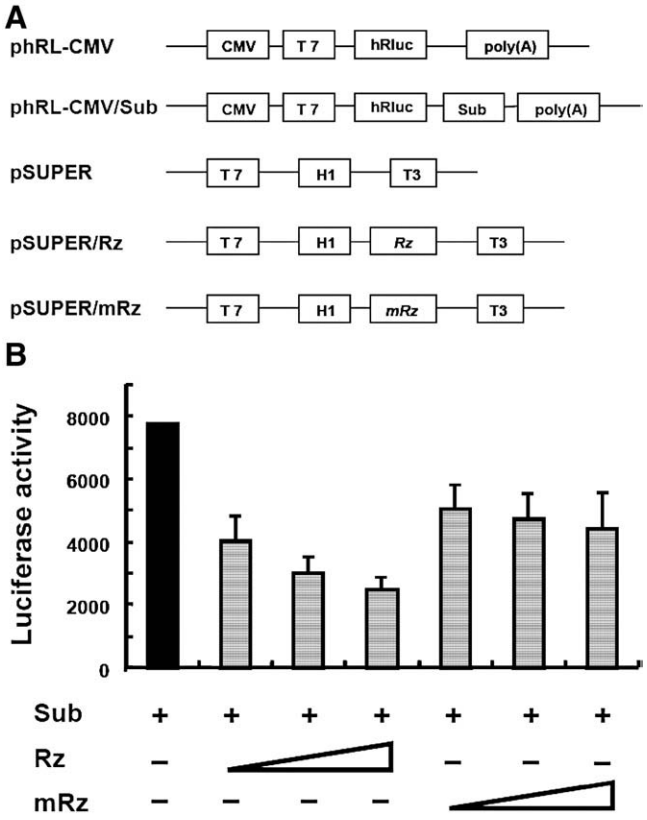

Fig. 3. Ribozyme intracellular cleavage assays. A: Schematic representation of the Sub reporter vector phRL-CMV/Sub and ribozyme producing vectors pSUPER/Rz and pSUPER/mRz. Sub sequence was inserted immediately before the poly(A) site of the *Renilla* gene and expression of ribozymes were driven by H1 promoter in pSUPER vector. B: Luciferase reporter assays of ribozyme cleavage. phRL-CMV/Sub was cotransfected with increasing amounts of pSUPER/Rz or pSUPER/mRz and *Renilla luciferase* activities were measured as the index of ribozyme activities.

VEGF reporter activity (Fig. 4A, bottom panel). This result strongly indicated that HIF-1α ribozyme could target its endogenous substrate and effectively block its responsive VEGF gene expression.

2.3. Efficacy of HIF-1α ribozyme in the xenograft tumors

Measurement of in vivo efficacy of exogenously delivered HIF-1α ribozyme was performed in xenograft nude mice (see Material and methods). Large tumors (approximately 3 mm in diameter) were formed before the synthetic Rz was injected subcutaneously surrounding the solid tumor every 3 days for 4 weeks because we reasoned that this regimen might reflect the clinical situation more closely where early diagnosis of cancers is often impractical. Compared to the mock treatment with PBS, Rz injection led to suppression of tumor growth in the fixed time frame of 28 days (Fig. 5A and 5B). Immunohistologic staining of the vascular endothelium indicated that the intratumoral administration of the ribozyme also inhibited angiogenesis as revealed by reduced tumor microvessel density (Fig. 5B and 5C). The new vessels in HeLa tumors also demonstrated decreased thickness of vascular endodermis (Fig. 5B), suggesting endothelial apoptosis might occur in response to down-regulation of HIF-1α. Finally, inhibition of tumor growth and antiangiogenesis by local administration of ribozyme directly correlated with the reduced expression of HIF-1α and VEGF as verified by reverse transcription PCR (Fig. 5E). The finding that Rz could effectively attenuate the tumor growth even after the tumor nodules reached 5 to 10 mm^3 (roughly 3 mm in diameter) was reminiscent of previous studies using antisense HIF-1α against EL-4 tumors with their sizes reaching 4 mm in diameter [28].

3. Materials and methods

3.1. Cell lines and reagents

HEK293T and HeLa cell lines were routinely maintained in DMEM (HyClone; Logan, UT) medium supplement with 10% fetal bovine serum (HyClone), 100 U/mL of penicillin, and 100 mg/mL of streptomycin at 37°C in 5% CO_2.

Restriction enzymes were all obtained from New England Biolabs, Riboprobe® in vitro Transcription Systems and Dual-Luciferase® Reporter Assay System were purchased from Promega, and Lipofectamine was from GIBCO. Plasmid DNA used in transient transfection was prepared using Maxiprep DNA Purification kits (Qiagen; Germany). $CoCl_2$ and all other fine chemicals were purchased from Sigma/Aldrich, U.S.A.

3.2. Plasmids

The RNA fragment spanning nt 1762-1778 of HIF-1α gene containing the GUC triplet was chosen as the template of ribozyme (Sub, Fig. 1). Sub RNA was either chemically synthesized (Dharmacon Research Inc, Lafayette, CO) or

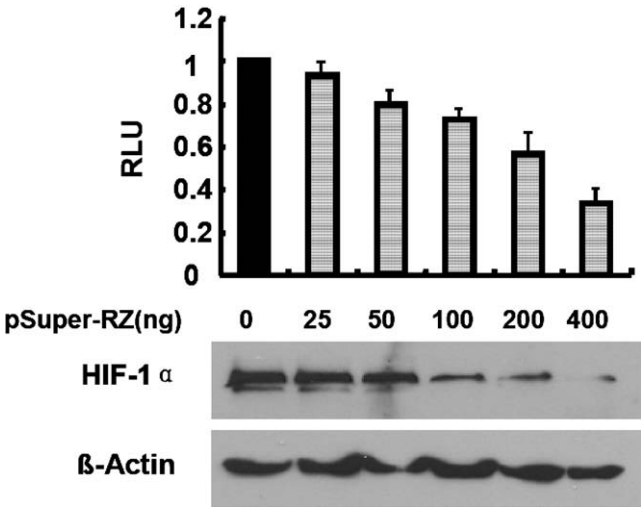

Fig. 4. The effect of the ribozyme on expression of HIF-1α under hypoxic conditions. HeLa cells were cotransfected with phRL-CMV/Sub and indicated amount of pSUPER-Rz, and *Renilla luciferase* activities under normoxic (blacked bar) or hypoxic (hatched bars) conditions were measured. In parallel, the expression levels of endogenous HIF-1α were assessed by Western blotting using a rabbit antiHIF-1α antibody. *β*-actin was detected as the protein loading control.

generated by in vitro transcription reaction from pSP72 (Riboprobe® in vitro Transcription Systems, Promega) that contained Sub encoding DNA sequence inserted between Xba I and Kpn I restriction sites (designated as pSP72-Sub). The cDNA sequence of Sub was also inserted to the *Renilla luciferase* gene before poly(A) in between Xba I and Not I sites in phRL-Luc vector (Promega; designated pCMV-hRL-Sub, Fig. 3). A firefly luciferase expression plasmid, pGL3-Luc (Promega), was used as an internal control of the cotransfection efficiency. The 38-mer complementary ribozyme (Rz, nucleotide sequence: 5′-CUAAUGGU*CUGAU GAGUCCGUGAGGACGAA*ACAACUGA-3′) containing the conserved catalytic domain (underlined), and its mutant variant (mRz, G11A point mutation in the boxed nucleotide) were designed that recognized 8 nucleotides of the substrate flanking GUC triplet in stems I and III (Fig. 1, "8 + 8" rule). The ribozymes were produced by in vitro transcription from pSP72 that contained corresponding ribozyme encoding DNA fragments inserted in between EcoR I and Bgl II. For in vivo cleavage experiments, Rz and mRz encoding DNA fragments were also subcloned in between Hind III and Bgl II restriction sites of pSUPER vector (OligoEngine; Seattle, WA; pSUPER-Rz and pSUPER-mRz; Fig. 3). The sequences and orientation of the inserts were verified by DNA sequence analysis.

The authentic VEGF promoter region (-1176 to +54 nt) containing HRE was cloned from a human genomic DNA clone and inserted upstream of the luciferase gene in pGL3-basic to yield pGL3-VEGF-Luc.

3.3. Ribozyme cleavage in vitro

Ribozyme and mRz ribozymes were produced by in vitro transcription reactions using T7 RNA polymerase after pSP72-Rz, pSP72-mRz, or pSP72-Sub was linearized with Xba I or EcoR I according to manufacturer's manual (Riboprobe® in vitro Transcription Systems, Promega). Substrate RNA (Sub) was internally labeled with 50 μCi ofα-^{32}P-CTP neuroendocrine neoplasm (NEN). The RNA transcripts were purified by denaturing polyacrylamide gel electrophoresis (PAGE) (8 mol/L urea) and quantified by UV spectrometry assuming a residue extinction coefficient at 260 nm of 6.6×10^{-3}/mol/L.cm as previously described [8]. Fixed amount of Sub (80 μmol/L) was mixed with increasing amount of Rz or mRz (240, 480, and 960 μmol/L) in a total volume of 10 μL of 50 mmol/L Tris-HCl (pH 7.5), denatured by heating at 95°C for 2 minutes, and slowly cooled to 37°C for 1 hour; the reaction was quenched on ice after addition of equal volume of the denaturing buffer (98% deionized formamide, 10 mmol/L EDTA (pH 8.0), 0.1% bromophenol blue, 0.1% xylene cyanol). Cleavage products were heated at 95°C for 2 minutes and resolved in 20% denaturing PAGE (8 mol/L urea) and quantitated by a PhosphoImager (Molecular Dynamics, U.S.A.).

3.4. Ribozyme cleavage in luciferase reporter assays

About 5×10^5 HEK293T cells were plated in 100 mm plates to reach 50% to 90% confluency overnight. About 2 ng pCMV-hRL/Sub and increasing amount of pSUPER-Rz or pSUPER-mRz (2, 160, 320 ng) were cotransfected into HEK293T cells using Lipofectamine according to manufacture's instructions. Plasmid pGL3-Luc (100 ng) was also included as an internal control of transfection efficiency, and the total DNA was normalized with various amount of empty vector pSUPER. Luciferase reporter activities were measured using the Dual-luciferase® Reporter μAssay System (Promega) with TD-20 luminometer (Turner Desings Instruments, U.K.). The RLU represented the average of 3 independent transfection assays normalized against the firefly luciferase activities. To measure the ribozyme activities under hypoxic conditions, 3×10^5 HeLa cells were plated into 6-well plates overnight for the confluence to reach approximately 70%. Fixed amount of reporter pGL3-VEGF-Luc plasmid (400 ng) was cotransfected with increasing amount of pSUPER-Rz plasmid (0, 25, 50, 100, 200, and 400 ng), and 1 ng of pCMV-hRL was included to normalize the transfection efficiency using Lipofectamine Plus (Invitrogen, Carlsbad, CA). The total amount of DNA was kept constant by adding the appropriate amount of the empty vector pSUPER. Ten hours posttransfection, freshly prepared $CoCl_2$ solution (3 mmol/L in stock) was added to the medium to reach the final concentration of 100 μm. Transfectants were incubated further for 38 hours before harvest for measurement of luciferase activity and HIF-1α expression by immunoblotting.

3.5. Western blot

The hypoxic HeLa transfectants were harvested and lysed in Radio Immunoprecipitation Assay (RIPA) buffer (50 mmol/L Tris-HCl [pH 7.5], 150 mmol/L NaCl, 0.1% SDS, 0.5% sodium cholate, 2 mmol/L EDTA, 1% NP-40, and 10% glycerol) containing the protease inhibitors cocktail (Complete, Roche, Basel, Switzerland) and 1 mmol/L Phenylmethanesulfonyl fluoride (PMSF) on ice for 30 minutes. Forty-five micrograms of whole cell lysate were mixed resolved in 8% Sodium dodecyl sulfate (SDS)-PAGE, and the expression level of HIF-1α was immunoblotted with the specific antibody (H-206, 1:150 in Phosphate Buffer Solution containing 0.05% Tween-20 [PH 7.40] (PBST)/1% milk, Santa Cruz, CA) and quantitated with chemiluminescence detection kit (ECL) (Pierce, Minneapolis, MN).

3.6. RNA antitranscription-PCR

Total tumor tissue RNA was extracted with Trizol reagents according to manufacturer's manual (Invitrogen). The first and second strand complementary DNA synthesis was carried out exactly as instructed by the manufacturer. The oligo DNA primer pairs were as follows: HIF-1α, 5′-GTCCAGATGG-TAGCGAC-3′ and 5′-GTGGGCCGTCCAACTTCC-3′; VEGF, 5′-GGACCCTGGCTT TACTGC-3′ and 5′-CGGG-CTTGGGCGATTTAG-3′; and β-actin, 5′-GTCGACAACG-GCTCCGGC-3′ and 5′-GGTGTGGTGCCAGATTTTCT-3′. The

PCR amplification conditions were 94°C, 4 minutes for one cycle, 28 cycles of 94°C for 30 seconds, 58°C for 45 seconds, and 72°C for 1 minute. The final round was 72°C for 8 minutes. The PCR products were analyzed on a 2% agarose gel.

3.7. Tumor regression by HIF-1α ribozyme in xenograft nude mice

The male athymic Balb/c nude mice were purchased from the National Institute for the Control of Pharmaceutical and

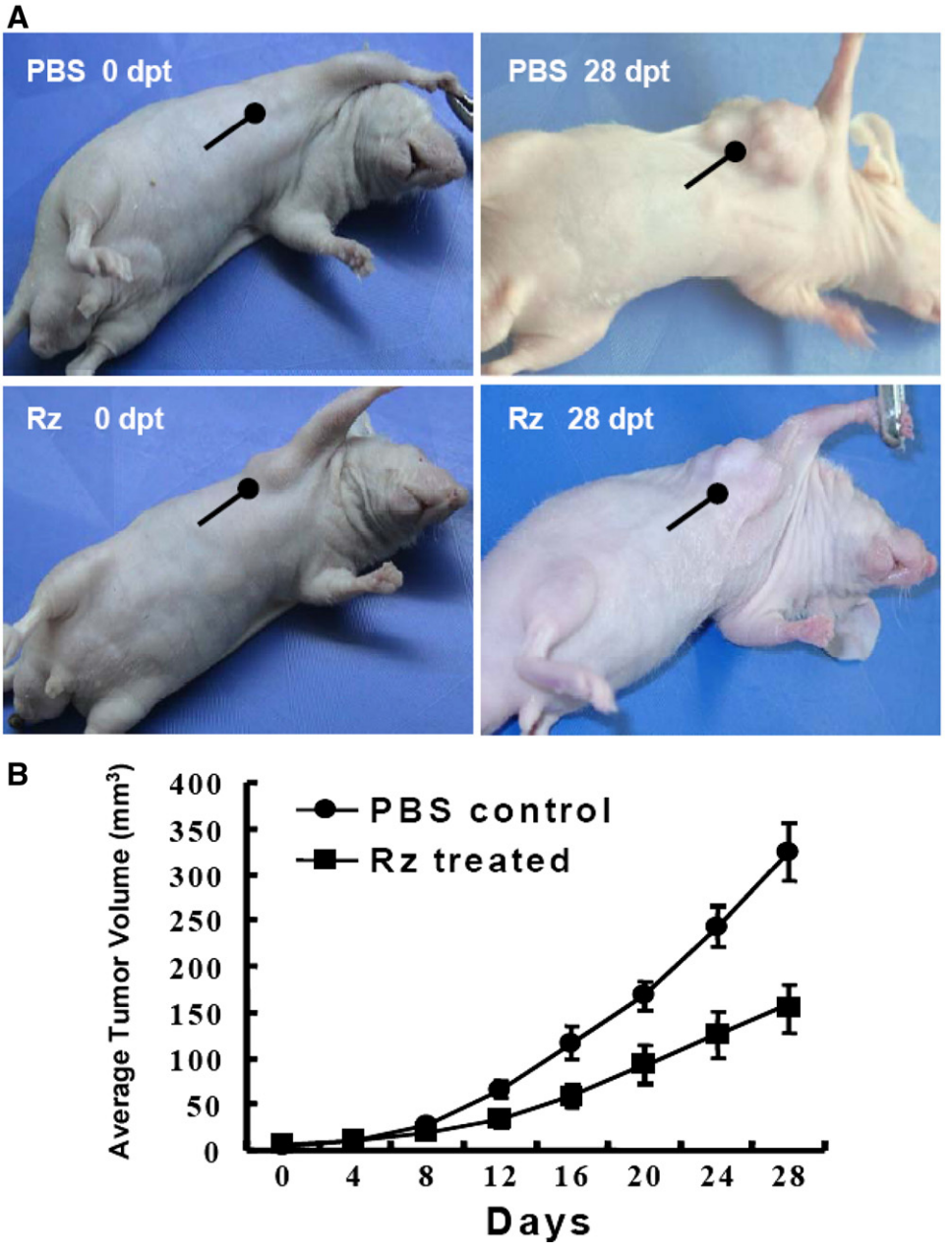

Fig. 5. Histopathologic determination and immunohistochemistry of HeLa tumors grown in nude mice. A: Viable HeLa cells (5×10^6) were injected subcutaneously into the axilla of female nude mice. After the tumors reached 100 to 150 mm^3 in size (0 day posttreatment, 0 dpt), mice received a local injection of Rz or PBS every 3 days for 4 weeks (28 dpt). B: Tumor growth was represented by the tumor sizes that were measured every 4 days with a caliper, and the volume was calculated by the formula (length × width × height) π/6. Data for Rz (n = 5) and PBS (n = 5) were presented as mean tumor volume ± SEM. Analysis of covariance of repeated measurement data test performed on the day 28, given $P < .05$ ($P = .031$) for the comparison between treated and control groups. C: Tumor sections were prepared one day after the last treatment and stained with hematoxylin and eosin (100×, top panel) or processed for immunohistochemical staining with an antifactor VIII-related antigen antibody to detect endothelial cells (200×, bottom panel). Arrows indicated the positions of vascula. D: Measurement of tumor vascularity. The tumor blood vessels stained with the antifactor VIII-related antigen antibody were counted in blindly chosen random fields to record per surface area (0.155 mm^2). A significant difference in mean vessel counts between HeLa tumors treated with Rz vs PBS ($P < .05$) is donated by stars. E: The VEGF and HIF-1α mRNA levels of tumor xenografts treated with Rz or PBS were analyzed by semiquantitative RT-PCR. Expression levels of β-actin were assessed as a loading control.

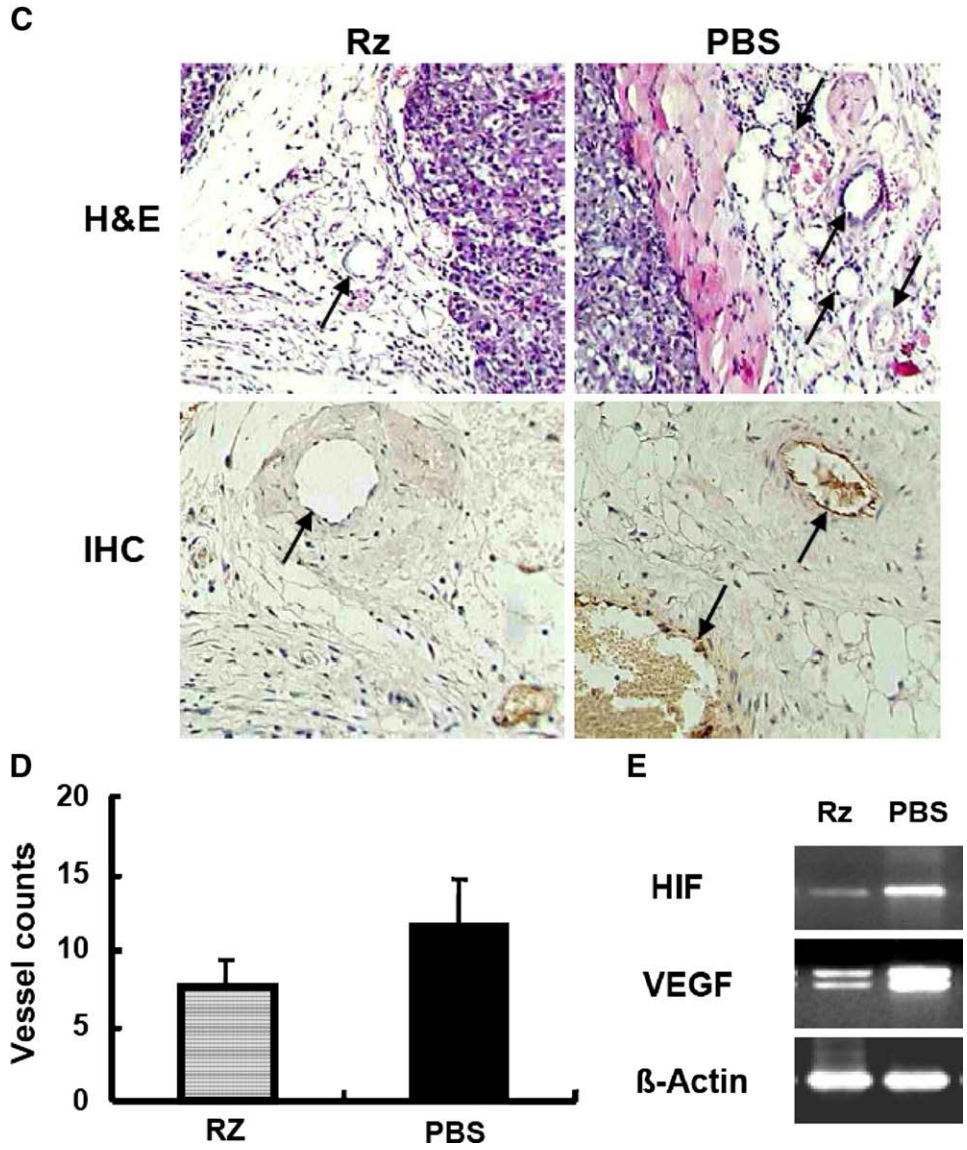

Fig. 5 (*continued*)

Biological Products (NICPBP), Beijing, China, and were housed under specific pathogen free (SPF) conditions. Single-cell suspension of 5×10^6 HeLa cells (>95% viability by trypan blue exclusion) in 0.1 mL of PBS was injected subcutaneously into the axilla of nude mice (n = 10). After the tumors reached approximately 10 mm^3 (approximately 3 mm in perpendicular diameters) in size, 5 mice received a local injection of the synthetic Rz (100 pmol Rz/g body weight of mice) mixed with Oligofectamine (GIBCO) in Opti-MEM1, and 5 received only PBS, once every 3 days for 4 weeks. One day after the last treatment, the mice were killed, and the tumors excised. The tissue was divided into 2 parts—one part was fixed with formalin and embedded in paraffin, the others were quickly frozen in liquid nitrogen and kept at −80°C until used.

3.8. Immunohistochemistry

After the last injection of Rz or PBS, HeLa tumors were removed and fixed with formalin and embedded in paraffin. Cryosections (6 μm) were stained either with hematoxylin and eosin or immunochemically stained for the endothelial cell marker factor VIII-related antigen to measure the microvascular density. In brief, the sections were deparaffinized, rehydrated, and digested by 0.05% trypsin for 20 minutes to retrieve the antigen. Nonspecific sites were blocked with PBS/2.5% bovine serum albumin for 1 hour and immunoblotted with rabbit antifactor VIII-related antigen polyclonal antibody (Dako Biotech, Kyoto, Japan; 1:50 dilution in the blocking solution) at 4°C overnight. 3,3′-diaminobenzidine tetrahydrochloride was used as the final chromogen. All immunostained sections were lightly counterstained with Mayer's hematoxylin before mounting.

3.9. Statistical analysis

Tumor size was measured every 4 days with a caliper, and the tumor volume was calculated by the formula (length × width × height) $\pi/6$ because of the irregular shape of the

tumor nodules, especially at the late stage of experiments. Data for each group (n = 5) were presented as mean tumor volume ± SEM. Analysis of covariance of repeated measurement data test was performed at 28 days post-Rz or mock treatment. Microvessel densities were analyzed using the Mann-Whitney U test, and $P < .05$ were considered as significant differences adapted from previously described method [21].

4. Discussion

With the advance of functional genomics and the shift of interest toward sequence-based therapeutics, intense research efforts have been taken on nucleic acid-mediated gene regulation technologies. In this study, we embarked on the ribozyme strategy to specifically target HIF-1α that is very much involved in tumorigenesis and angiogenesis. We were able to demonstrate that the ribozyme could specifically cleave its HIF-1α substrate RNA in a dose-dependent fashion both in vitro and in vivo, indicating that most likely the selected accessible target site and design of corresponding hammerhead ribozyme that function in trans to down-regulate HIF-1α expression might be feasible. More interesting, administration of the synthetic ribozyme into tumor xenografts showed promising tumor regression and suppressed angiogenesis. While the particular administration regimen of the catalytic RNA in this study could not completely eradicate the tumor or reduce the solid tumor to microscopic dormant nodules, partly because of a relatively large tumor size to begin with, intensive investigation of the ribozyme into more efficient nucleic acid delivery and more favorable catalytic kinetics and thermodynamics under physiologic conditions would potentially yield a therapeutically potent antiangiogenesis agent.

A successful ribozyme strategy deals with the accessible substrate site selection, optimal rybozymatic activity, and efficient delivery [2,19]. Limited predictability of target site selection models is recognized as one major stumbling block of the so-called complementary technologies. Beside the traditional computer-assisted site selection of the target RNA using Mfold program [35,36], currently used in vitro systems for target site selection include RNAse H-based mapping, antisense oligonucleotide microarrays, and functional screening approaches using libraries of catalysts with randomized target-binding arms to identify optimal ribozyme/DNAzyme cleavage sites [2]. We used a similar computational secondary structure prediction of HIF-1α RNA [3] with the advantage of the capacity of predicting optimal or suboptimal target motifs of a long RNA substrate. One of the 3 target sites selected seemed to be an accessible one in both in vitro and in vivo experiments.

It is intriguing to observe that injection of HIF-1α ribozyme RNA with oligofectamine could effectively attenuate the growth and angiogenesis of the established large HeLa tumors. Failure of mice to completely reject tumors was reminiscent of a similar approach by using antisense HIF-1α against large EL-4 tumors after reaching 4 mm in diameter [28]. However, our results differed from the antisense results in that only partial inhibition of HIF-1α expression was achieved by using the ribozyme, maybe because of nonoptimal potency and selectivity for the designed ribozyme in the natural physiologic environment. On the other hand, complete inhibition of HIF-1α by antisense vector [28] yielded a similar attenuation of tumors to that of ribozyme treatment in this study suggests that ribozyme might still be a preferred approached considering its improved target/effector stoichiometry as compared with antisense oligonucleotides of the same specificity. Of course, there is no direct comparison between 2 different tumors for their response to HIF-1α; nevertheless, both studies strongly indicated that knockdown expression of HIF-1α could be a suitable therapeutic means to contain or curb tumor progression. Considering that complex mechanisms are involved in tumorigenesis and metastasis and combination of HIF-1α antisense targeting and immunotherapy or chemotherapy could effectively eliminate large tumors [28,29], combination therapy for ribozyme against HIF-1α with chemotherapy against multiple tumor survival and angiogenesis would be an approach of choice.

As similar to other antisense RNA and ribozymes approaches, HIF-1α ribozyme still face the problems of lacking a physiologic selection system to rapidly determine suitable nucleic acid compounds for therapeutic applications. Extensive studies of HIF-1α ribozyme to optimize the physiologic parameters, such as annealing reactions, duplex stability, and ribozymatic catalysis, as well as efficient RNA oligo delivery, are under investigation.

Acknowledgment

This work was supported by grants from One Hundred Scholars Fellowship of Chinese Academy of Sciences, Beijing, China MOST 973 (2002CB513001) and NSFC Outstanding Young Investigator Fellowship, Beijing, China (30025010) (H Tang) and Key Projects of Jiangsu Province Health Department, Nanjing, China (H200104) (R Yu).

References

[1] Aebersold DM, Burri P, Beer KT, et al. Expression of hypoxia-inducible factor-1alpha: a novel predictive and prognostic parameter in the radiotherapy of oropharyngeal cancer. Cancer Res 2001;61:2911-6.

[2] Bramlage B, Luzi E, Eckstein F. Designing ribozyme for the inhibition of gene expression. Trends Boitechnol 1998;16:434-8.

[3] Brodsky LI, Ivanov VV, Kalaidzidis YaL, et al. GeneBee-NET: internet-based server for analyzing biopolymers structure. Biochemistry 1995;60:923-8.

[4] Bruick RK. Oxygen sensing in the hypoxic response pathway: regulation of the hypoxia-inducible transcription factor. Genes Dev 2003;17:2614-23.

[5] Carmeliet P, Dor Y, Herbert JM, et al. Role of HIF-1alpha in hypoxia-mediated apoptosis, cell proliferation and tumour angiogenesis. Nature 1998;394:485-90.

[6] Cech TR. Self-splicing of group I introns. Annu Rev Biochem 1990; 59:543-68.
[7] Dai S, Huang ML, Hsu CY, et al. Inhibition of hypoxia inducible factor 1alpha causes oxygen-independent cytotoxicity and induces p53 independent apoptosis in glioblastoma cells. Int J Radiat Oncol Biol Phys 2003;55:1027-36.
[8] Fedor MJ, Uhlenbeck OC. Kinetics of intermolecular cleavage by hammerhead ribozymes. Biochemistry 1992;31:12042-54.
[9] Forsythe JA, Jiang BH, Iyer NV, et al. Activation of vascular endothelial growth factor gene transcription by hypoxia-inducible factor 1. Mol Cell Biol 1996;16:4604-13.
[10] Giaccia A, Siim BG, Johnson RS. HIF-1 as a target for drug development. Nat Rev Drug Discov 2003;2:803-11.
[11] Harris AL. Hypoxia—a key regulatory factor in tumour growth. Nat Rev Cancer 2002;2:38-47.
[12] Haseloff J, Gerlach WL. Simple RNA enzymes with new and highly specific endoribonuclease activities. Nature 1988;334:585-91.
[13] Hockel M, Vaupel P. Tumor hypoxia: definitions and current clinical, biologic, and molecular aspects. J Natl Cancer Inst 2001;93:266-76.
[14] Iyer NV, Kotch LE, Agani F, et al. Cellular and developmental control of O_2 homeostasis by hypoxia-inducible factor 1 alpha. Genes Dev 1998;12:149-62.
[15] Jiang BH, Rue E, Wang GL, et al. Dimerization, DNA binding, and transactivation properties of hypoxia-inducible factor 1. J Biol Chem 1996;271:17771-8.
[16] Kaelin Jr WG. How oxygen makes its presence felt. Genes Dev 2002; 16:1441-5.
[17] Krishnamachary B, Berg-Dixon S, Kelly B, et al. Regulation of colon carcinoma cell invasion by hypoxia-inducible factor 1. Cancer Res 2003;63:1138-43.
[18] Lieber A, Strauss M. Selection of efficient cleavage sites in target RNAs by using a ribozyme expression library. Mol Cell Biol 1995;15: 540-551.
[19] Puerta-Fernandez E, Romero-Lopez C, Barroso-delJesus A, et al. Ribozymes: recent advances in the development of RNA tools. FEMS Microbiol Rev 2003;27:75-97.
[20] Pugh CW, Ratcliffe PJ. Regulation of angiogenesis by hypoxia: role of the HIF system. Nat Med 2003;9:677-84.
[21] Ryan HE, Lo J, Johnson RS. HIF-1 alpha is required for solid tumor formation and embryonic vascularization. Embo J 1998;17: 3005-15.
[22] Semenza GL. HIF-1 and mechanisms of hypoxia sensing. Curr Opin Cell Biol 2001;13:167-71.
[23] Semenza GL. HIF-1 and human disease: one highly involved factor. Genes Dev 2000;14:1983-91.
[24] Semenza GL. Regulation of hypoxia-induced angiogenesis: a chaperone escorts VEGF to the dance. J Clin Invest 2001;108:39-40.
[25] Semenza GL. Targeting HIF-1 for cancer therapy. Nat Rev Cancer 2003;3:721-32.
[26] Semenza GL, Wang GL. A nuclear factor induced by hypoxia via de novo protein synthesis binds to the human erythropoietin gene enhancer at a site required for transcriptional activation. Mol Cell Biol 1992;12:5447-54.
[27] Shimayama T, Nishikawa S, Taira K. Generality of the NUX rule: kinetic analysis of the results of systematic mutations in the trinucleotide at the cleavage site of hammerhead ribozymes. Biochemistry 1995;34:3649-54.
[28] Sun X, Kanwar JR, Leung E, et al. Gene transfer of antisense hypoxia inducible factor-1 alpha enhances the therapeutic efficacy of cancer immunotherapy. Gene Ther 2001;8:638-45.
[29] Sun X, Kanwar JR, Leung E, et al. Regression of solid tumors by engineered overexpression of von Hippel-Lindau tumor suppressor protein and antisense hypoxia-inducible factor-1alpha. Gene Ther 2003;10:2081-9.
[30] Symons RH. Self-cleavage of RNA in the replication of small pathogens of plants and animals. Trends Biochem Sci 1989;14:445-50.
[31] Talks KL, Turley H, Gatter KC, et al. The expression and distribution of the hypoxia-inducible factors HIF-1alpha and HIF-2alpha in normal human tissues, cancers, and tumor-associated macrophages. Am J Pathol 2000;157:411-21.
[32] Unruh A, Ressel A, Mohamed HG, et al. The hypoxia-inducible factor-1 alpha is a negative factor for tumor therapy. Oncogene 2003;22: 3213-20.
[33] Wang GL, Jiang BH, Rue EA, et al. Hypoxia-inducible factor 1 is a basic-helix-loop-helix-PAS heterodimer regulated by cellular O2 tension. Proc Natl Acad Sci U S A 1995;92:5510-4.
[34] Zhong H, De Marzo AM, Laughner E, et al. Overexpression of hypoxia-inducible factor 1alpha in common human cancers and their metastases. Cancer Res 1999;59:5830-5.
[35] Zuker M. On finding all suboptimal foldings of an RNA molecule. Science 1989;244:48-52.
[36] Zuker M, Stiegler P. Optimal computer folding of large RNA sequences using thermodynamics and auxiliary information. Nucleic Acids Res 1981;9:133-48.

Commentary

The authors provide a very well-documented study with all the experiments clearly indicating the strong role of HIF-1α gene and angiogenesis. Early studies have revealed that both HIF-1 expression and Stat3 activity are up-regulated in diverse cancers. In vitro and in vivo studies were also done with respect to Stat3 and VEGF expression and their significant role in angiogenesis. It should be noted HIF-1α is not the only target, but this gene could be an important one on which to focus.

Radhika Gade Andavolu, PhD
Genetic Research Institute of the Desert
Rancho Mirage, CA 92270, USA